JGP Journal of General Physiology

COMMENTARY

Just how many holes...?

Gyorgy Csordas and Stephen Hurst

The mitochondrial inner membrane (IMM) is loaded with membrane proteins, most of which are directly or indirectly involved in ion transport. As the powerhouses of the cell, mitochondria are platforms for massive energy transformations and/or transduction. The chemical energy derived from oxidative nutrient metabolism is transduced to electric potential ($\Delta\Psi_m$) across the extensively folded IMM, which then drives cations to the matrix with such a force that it reverses the H^+ pump F_1F_0-ATPase to operate as ATP synthase. Besides the protons, uptake and extrusion pathways also exist for Ca^{2+} as a signaling messenger but the mitochondrial matrix can also serve as a high-capacity low-affinity Ca^{2+} sink. Like a combustion engine power generator, mitochondria also catalyze intensive redox cycling, and imbalances in the use of fuel, oxidizing medium, and the power generated may cause "engine overheating," damage, or failures that can be prevented by various safety features. One of the most ominous and dramatic safety features of these semi-autonomous organelles is connected to the self-defense against toxic Ca^{2+} overload and against accumulation of reactive oxygen species (ROS): the mitochondrial permeability transition (mPT). Ca^{2+} homeostasis in the mitochondrial matrix is governed mostly by the highly selective and tightly gated mitochondrial Ca^{2+} uniporter channel complex (MCUC) as the uptake route, while Na^+ and/or H^+ exchangers serve as the route of Ca^{2+} egress. At rest, in nonexcitable cells, the MCUC cytosolic $[Ca^{2+}]$ activation threshold is rarely crossed, mostly by local "elementary" Ca^{2+} signaling events (e.g., $[Ca^{2+}]$ puffs), and the resulting transient mitochondrial Ca^{2+} uptake and mitochondrial matrix $[Ca^{2+}]$ ($[Ca^{2+}]_m$) signal is fully cleared by the exchangers. If Ca^{2+} uptake surpasses the extrusion, Ca^{2+} will be retained in the matrix. Usually, the Ca^{2+} retention capacity is much larger than the Ca^{2+} amount required for maximum $[Ca^{2+}]_m$ signal (Chalmers and Nicholls, 2003), owing to the formation of Ca^{2+} phosphate precipitates and some other, less defined chelation mechanisms. However, the effective mitochondrial Ca^{2+} retention capacity is less than what the matrix can accommodate: it is capped by a regulated "safety valve," which is the formation and activation of the mPT pore (mPTP). The mPTP operates as a "great equalizer" in the form of a nonselective aqueous pore, allowing passage for ions and solutes with an average molecular weight cutoff of 1.5 kD (Haworth and Hunter, 1979). While short-term activation of such a safety valve could reset Ca^{2+}-overloaded or -overcharged (e.g., hyperpolarized, ROS over-generating) mitochondria, sustained mPTP opening is deleterious at multiple levels, bringing about matrix swelling to the extent that quasi "ruptures" form in the outer mitochondrial membrane (OMM). Proapoptotic proteins are then liberated from the intermembrane space, initiating the process of mitochondrial apoptosis or regulated necrotic cell death.

Although mPTP has been known for 40 yr, both its formation and activation properties have been under intense scrutiny and unsettled debate even in present days. Intriguingly, the proteins primarily suspected in constituting mPTP, the ATP/ADP carrier (adenine nucleotide translocator [ANT]; Karch et al., 2019), possibly together with the phosphate carrier (PiC; Richardson and Halestrap, 2016), and the F_1F_0-ATPase (Mnatsakanyan et al., 2019; Urbani et al., 2019) are all highly abundant membrane proteins. This of course raised the question of how big of a portion of these proteins would contribute to mPTP.

In this issue of the *Journal of General Physiology*, Evgeny Pavlov's group (Neginskaya et al., 2020) have taken on the difficult task of assessing the quantity of mPTPs in mitoplasts (isolated from mouse livers) subjected to Ca^{2+} overloading. The main idea for the assessment strategy was to use the rate of mPTP-associated swelling as a readout of water influx via the mPTP. Based on approximative modeling of mPTP with carbon nanotubes, they predicted the unitary water flux (j_{PTP}) as 0.65×10^{-18} kg/s flow per 1 mOsm of driving pressure. The bacterial pore-forming toxin α-hemolysin has been known to have similar unitary conductance to the mPTP, and the unitary water flux for α-hemolysin has been experimentally determined as $\sim 1.5 \times 10^{-12}$ cm^3/s or $\sim 1.5 \times 10^{-15}$ kg/s (Paula et al., 1999). After normalizing to the osmotic pressure, this unitary water flux is at a similar order as the one calculated for the mPTP, thus strengthening confidence in the approximation. The total water flux per whole mitoplast was determined based on the rate of swelling (volume increase) after the OMM rupture, when it was only limited by

MitoCare Center for Mitochondrial Imaging Research and Diagnostics at the Department of Pathology, Anatomy and Cell Biology, Thomas Jefferson University, Philadelphia, PA.

Correspondence to Gyorgy Csordas: Gyorgy.Csordas@jefferson.edu.

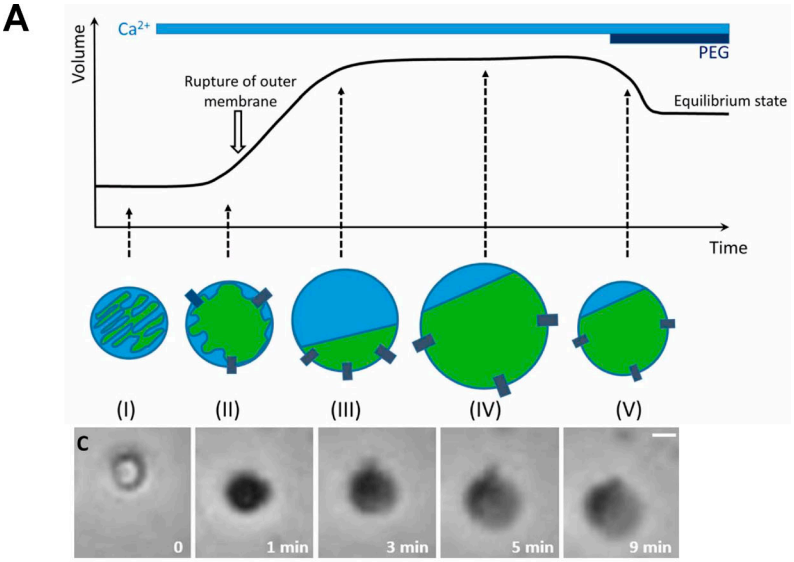

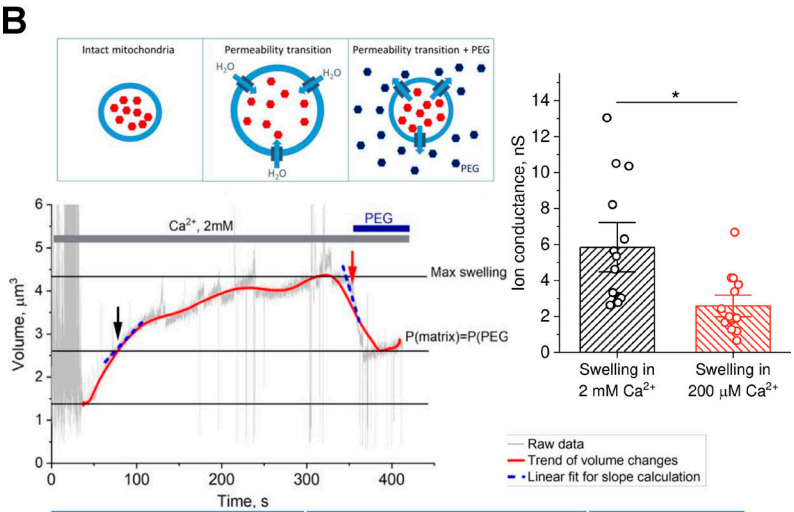

Extramitochondrial Ca^{2+}	Conductance (nS) (Min, Max, Avg)			Active Pores
2 mM Ca^{2+}	2.6	13.1	5.9	1.7 - 8.7
200 µM Ca^{2+}	0.7	6.7	2.6	0.5 - 4.5

Figure 1. **Experimental plan to quantify the number of open mPT Pores. (A)** Energized mitochondria (I), when overloaded with Ca^{2+}, trigger mPTP opening (II), and due to oncotic forces undergo matrix swelling to the point of rupturing the outer mitochondrial membrane (III), then enlarging until the IMM elastic force reaches equilibrium (IV), which can be equilibrated through addition of impermeable (>1.5 kD) PEG. **(B)** The rate of mitoplast volume change was used to determine the total flux of water, which was then normalized by oncotic pressure. This, divided by the estimated flux per 2 nm mPT pore, yielded the number of pores per mitoplast. Ion conductance was calculated using a value of 1.5 nS per pore. Panels and data are from Neginskaya et al. 2020.

the oncotic pressure difference across the IMM, hence it was reversible by addition of high-molecular weight polyethylene glycol (PEG 8000; Fig. 1). Dividing the total water flux with the unitary flux provided the estimate of mPTP copy number in the mitoplast. In control assays, it was demonstrated that the water intake through the IMM during swelling during the transition from the "condensed" to the "orthodox" matrix conformation in the absence of substrates (Hackenbrock, 1966) is not affected by the externally applied oncotic pressure exerted by PEG in the recorded time frame. This validation also suggests that the mPTP-mediated water passage is overwhelmingly greater than the other water transport pathways across the IMM. The authors complemented the swelling-based assays with patch clamp recordings in patches from mitoplasts excised after mPTP activation and swelling.

The results of these assays depicted a stark contrast between the high abundance of the proposed mPTP constituents ANT and F_1F_0-ATPase and the active mPTP copy number per mitoplast, which turned out to be very low: <10 mPTP at 2 mM [Ca^{2+}] and <5 mPTP at 200 µM [Ca^{2+}]. The water flux calculations on one hand were conservative by using the smallest reported pore diameter (2 nm), while on the other hand the mPTP was approximated by molecular dynamics simulations of pristine carbon nanotubes, which conduct water better than carbon nanotubes with more polar pore lining (Casanova et al., 2019). However, even after correcting to this difference, the predicted copy number is still very low, considering the estimated >10^4 copies of ANT and likely several hundred or thousand copies of ATP synthase (based on proteomic data from yeast; Morgenstern et al., 2017).

Only so few... Why and how?

Although this is not the first time that a low copy number for the mPTP is proposed (e.g., a relative assessment was made based on inhibitor binding assays by the Halestrap group; Richardson and Halestrap, 2016), this is the first systematic quantitative assessment of the absolute copy number. Of course, this outcome raises (or revives) several old and new questions in mitochondrial biology/physiology. Probably the most outstanding question is why and how so few mPTPs assemble from such large pools of constituents like ANT, PiC, or ATP synthases. What could be the limiting factors of the assembly besides a potential autolimitation in the progression posed by the massive rearrangements, homeostatic and energetic collapse, and IMM ballooning past the point of OMM rupture? By simple logic, either or both a small portion of ANT, PiC, and relevant F_1F_0-ATPase complexes must be structurally different from the rest (e.g., posttranslational modifications, protein–protein interactions) and/or the coincidence of multiple factors that lead to mPTP formation/activation takes place only at distinct submitochondrial locations. Indeed, multiple proposed mPTP paradigms have involved protein–protein interactions at OMM–IMM contact sites (reviewed in Hurst et al., 2017). Traditionally, the homeostatic alterations in the matrix that promote mPTP (Ca^{2+} accumulation in the matrix, ROS, and depolarization) have been considered to diffusely and more or less homogenously expose the IMM. However, evidence has been accumulating recently that suggest submitochondrial heterogeneities and subcompartmentalization. In some cases, these heterogeneities occur as location bias for certain transport proteins or for the mitochondrial replication machinery in response to the local environment of the mitochondrion (e.g., at contacts with other organelles like sarcoplasmic/endoplasmic reticulum; Lewis et al., 2016). Also, individual mitochondria may functionally segment to zones with varying matrix content and $\Delta\Psi_m$ of individual cristae (Wolf et al., 2019), and openings of dilated cristae frequently face contact areas with the endoplasmic reticulum as places of local Ca^{2+}, redox, and ROS crosstalk (Booth et al., 2016).

Notably, in the Ca^{2+} uptake route through the IMM, MCUC also has been reported to have distribution biases. Multiple groups suggested a bias toward the inner boundary membrane or cristae junctions (Gottschalk et al., 2019; Wang et al., 2019), and we described MCUC hotspot formation in the cardiac muscle mitochondria at the contacts with the junctional sarcoplasmic reticulum, which are local Ca^{2+} signal exposure sites (De La Fuente et al., 2016). Potential interaction and/or coclustering of the MCUC and the mPTP have also been proposed, possibly via connection of mPTP and MCUC through MCUR1 (Chaudhuri et al., 2016), or more recently, via potential direct interaction between MCU and F_1F_0-ATPase c-subunit transmembrane domains (Huang and Docampo, 2020).

Another interesting outcome of this study has been the dependence of the estimated mPTP copy number on the extramitochondrial $[Ca^{2+}]$: more mPTPs were predicted to be active at 2 mM $[Ca^{2+}]$ than at 200 µM $[Ca^{2+}]$. Both of these concentrations, when sustained, fall in the range that causes PT. It is tempting to speculate that the speed of mitochondrial Ca^{2+} uptake, the consequent depolarization, or the $[Ca^{2+}]_m$ dynamics in the immediate vicinity of MCUC may have a role in controlling the mPTP number (Fig. 2). The $K_{[Ca^{2+}]}$ found for MCUC activation in whole-mitoplast patch-clamp studies was very high (19 mM); this suggests that the MCUC would not be saturated even at 2 mM $[Ca^{2+}]$, although the mitochondrial Ca^{2+} uptake would be progressively hindered by the IMM depolarization due to the cation influx (Kirichok et al., 2004). To this end, it will be interesting to see follow-up studies performing similar mPTP copy estimates for mitochondria of different tissues: MCUC activation in the liver is known to be highly cooperative while, for example, in the heart it is less cooperative owing to different stoichiometry of MCUC components (MICU:MCU ratio; Paillard et al., 2017). Regarding tissue-specific differences, there is also great heterogeneity in the size, shape, and structural complexity (e.g., cristae) of mitochondria among tissues. It will be interesting to correlate these differences in copy number under normal conditions and conditions associated with altered mitochondrial dynamics (especially fusion/fission balance and cristae biogenesis).

Perspectives and limitations

From the key homeostatic imbalances leading to mPTP formation/activation, the Neginskaya et al. (2020) study focuses on Ca^{2+} overload. It will be important to follow up how other triggers like ROS/oxidative stress regulate mPTP number. It will also be useful to further confirm some of the approximations, such as the unitary water flux through the mPTP, as well as find ways to enhance the accuracy in the volume assessment of individual mitochondria (e.g., using higher resolution or super-resolution imaging).

Another potential limitation is that the study relies on the mPTP-mediated matrix swelling following the rupture of the OMM. This event reportedly has the requirement of an interaction with apoptotic pore-forming proteins in the OMM, Bax, and/or Bak, but these proteins are not needed for mPTP formation (Karch et al., 2013). Whether mPTP would indeed form a (super)complex with Bax/Bak oligomers in the OMM has not been established; however, mPTP is strongly desensitized in Bax/Bak DKO cells (Karch et al., 2013), and direct interaction between Bax/Bak and ANT have been reported by multiple groups (Marzo et al., 1998; Narita et al., 1998). If the direct interaction of mPTP with OMM proteins was a sensitizing factor, one would expect the mPTP in the free IMM of the mitoplast to behave differently (e.g., more time at low subconductances) from the one at the remaining contacts with the ruptured OMM. Accordingly, calculating with maximum conductance (or unitary water flux) for all mPTPs may be, to some extent, an underestimation of the total number of mPTPs, but an overestimation of the number of fully open pores. Indeed, the rapid reversal of the swelling happened only when the external oncotic pressure was increased using PEG of 2000 D but not 400 D, which passes through the fully open pores. However, a slower transient shrinkage at the beginning of PEG 400 D addition likely reflected a pool of partially open mPTPs that allowed in water but not the PEG (Fig. 8 in Neginskaya et al., 2020).

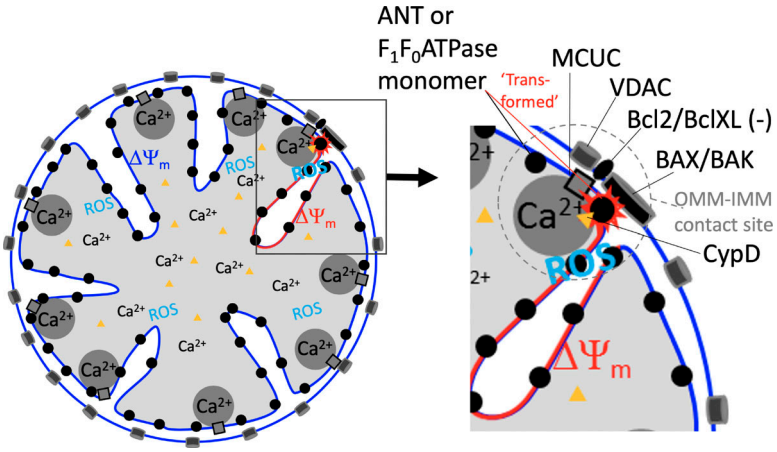

Figure 2. **Molecular, homeostatic, and structural coincidences in the mPTP formation.** Hypothetical scheme to illustrate how only a few of the otherwise abundant pore-building constituents form the mPTP. Although mitochondria are full of the main (most established) PT pore components, ANT and F_1F_0-ATPase, they transform to mPTP only at the right place and right time under specific circumstances. Without listing all components, some of the main coincidence factors proposed to drive the mPTP formation are shown in the scheme: the pore component at an OMM–IMM contact site may be exposed to high local [Ca^{2+}] next to MCUC for an extended time. The location is close to a cristae junction and the involved crista is depicted with locally altered ΔΨm (either hyperpolarization, producing more ROS, or depolarization as mPTP sensitizers). Recruitment of cyclophilin D (CypD) from the matrix is required as well as inputs from OMM-resident proteins, particularly the relatively low (compared with VDAC) number of oligomerized Bax/Bak. Besides (or as a result of) the coinciding factors, the 'chosen apo-constituents' will undergo the necessary transformation to form mPTP.

An important parameter, the number of pores during mitochondrial PT has thus been determined. How the key factors in mPTP formation/activation (e.g., Ca^{2+}, ROS, and pH) regulate this parameter can now be systematically evaluated, which will lead to better understanding of the dynamics of PT and, combined with genetic approaches, likely provide further clues to how individual molecular components might limit the mPTP copy number. This has been a great step toward the understanding of the mPTP copy requirement of the "terminal" PT. It is left for future studies to unravel how many copies and perhaps how many kinds of mPTPs operate to fulfill transient safety valve functions, manifested as mitochondrial "flashes," "flickers," and "mitowinks" that have been attributed to an increasing number of physiological processes including metabolism, wound healing, cellular differentiation, and stemness (reviewed in Hurst et al., 2017). It is also for later studies to elucidate if the mPTP that supports physiological pro-survival processes is a constitutive regulated-channel entity in the mitochondria or a conditional channel assembly.

Acknowledgments

Eduardo Ríos served as editor.

The authors declare no competing financial interest.

References

Booth, D.M., B. Enyedi, M. Geiszt, P. Várnai, and G. Hajnóczky. 2016. Redox Nanodomains Are Induced by and Control Calcium Signaling at the ER-Mitochondrial Interface. *Mol. Cell.* 63:240–248. https://doi.org/10.1016/j.molcel.2016.05.040

Casanova, S., M.K. Borg, Y.M.J. Chew, and D. Mattia. 2019. Surface-Controlled Water Flow in Nanotube Membranes. *ACS Appl. Mater. Interfaces.* 11:1689–1698. https://doi.org/10.1021/acsami.8b18532

Chalmers, S., and D.G. Nicholls. 2003. The relationship between free and total calcium concentrations in the matrix of liver and brain mitochondria. *J. Biol. Chem.* 278:19062–19070. https://doi.org/10.1074/jbc.M212661200

Chaudhuri, D., D.J. Artiga, S.A. Abiria, and D.E. Clapham. 2016. Mitochondrial calcium uniporter regulator 1 (MCUR1) regulates the calcium threshold for the mitochondrial permeability transition. *Proc. Natl. Acad. Sci. USA.* 113:E1872–E1880. https://doi.org/10.1073/pnas.1602264113

De La Fuente, S., C. Fernandez-Sanz, C. Vail, E.J. Agra, K. Holmstrom, J. Sun, J. Mishra, D. Williams, T. Finkel, E. Murphy, et al. 2016. Strategic Positioning and Biased Activity of the Mitochondrial Calcium Uniporter in Cardiac Muscle. *J. Biol. Chem.* 291:23343–23362. https://doi.org/10.1074/jbc.M116.755496

Gottschalk, B., C. Klec, G. Leitinger, E. Bernhart, R. Rost, H. Bischof, C.T. Madreiter-Sokolowski, S. Radulović, E. Eroglu, W. Sattler, et al. 2019. MICU1 controls cristae junction and spatially anchors mitochondrial Ca^{2+} uniporter complex. *Nat. Commun.* 10:3732. https://doi.org/10.1038/s41467-019-11692-x

Hackenbrock, C.R. 1966. Ultrastructural bases for metabolically linked mechanical activity in mitochondria. I. Reversible ultrastructural changes with change in metabolic steady state in isolated liver mitochondria. *J. Cell Biol.* 30:269–297. https://doi.org/10.1083/jcb.30.2.269

Haworth, R.A., and D.R. Hunter. 1979. The Ca2+-induced membrane transition in mitochondria. II. Nature of the Ca2+ trigger site. *Arch. Biochem. Biophys.* 195:460–467. https://doi.org/10.1016/0003-9861(79)90372-2

Huang, G., and R. Docampo. 2020. The Mitochondrial Calcium Uniporter Interacts with Subunit c of the ATP Synthase of Trypanosomes and Humans. *MBio.* 11. e00268-20. https://doi.org/10.1128/mBio.00268-20

Hurst, S., J. Hoek, and S.S. Sheu. 2017. Mitochondrial Ca^{2+} and regulation of the permeability transition pore. *J. Bioenerg. Biomembr.* 49:27–47. https://doi.org/10.1007/s10863-016-9672-x

Karch, J., J.Q. Kwong, A.R. Burr, M.A. Sargent, J.W. Elrod, P.M. Peixoto, S. Martinez-Caballero, H. Osinska, E.H. Cheng, J. Robbins, et al. 2013. Bax and Bak function as the outer membrane component of the mitochondrial permeability pore in regulating necrotic cell death in mice. *eLife.* 2. e00772. https://doi.org/10.7554/eLife.00772

Karch, J., M.J. Bround, H. Khalil, M.A. Sargent, N. Latchman, N. Terada, P.M. Peixoto, and J.D. Molkentin. 2019. Inhibition of mitochondrial permeability transition by deletion of the ANT family and CypD. *Sci. Adv.* 5. eaaw4597. https://doi.org/10.1126/sciadv.aaw4597

Kirichok, Y., G. Krapivinsky, and D.E. Clapham. 2004. The mitochondrial calcium uniporter is a highly selective ion channel. *Nature.* 427:360–364. https://doi.org/10.1038/nature02246

Lewis, S.C., L.F. Uchiyama, and J. Nunnari. 2016. ER-mitochondria contacts couple mtDNA synthesis with mitochondrial division in human cells. *Science.* 353. aaf5549. https://doi.org/10.1126/science.aaf5549

Marzo, I., C. Brenner, N. Zamzami, J.M. Jürgensmeier, S.A. Susin, H.L. Vieira, M.C. Prévost, Z. Xie, S. Matsuyama, J.C. Reed, et al. 1998. Bax and adenine nucleotide translocator cooperate in the mitochondrial control of apoptosis. *Science.* 281:2027–2031. https://doi.org/10.1126/science.281.5385.2027

Mnatsakanyan, N., M.C. Llaguno, Y. Yang, Y. Yan, J. Weber, F.J. Sigworth, and E.A. Jonas. 2019. A mitochondrial megachannel resides in monomeric F_1F_O ATP synthase. *Nat. Commun.* 10:5823. https://doi.org/10.1038/s41467-019-13766-2

Morgenstern, M., S.B. Stiller, P. Lübbert, C.D. Peikert, S. Dannenmaier, F. Drepper, U. Weill, P. Höß, R. Feuerstein, M. Gebert, et al. 2017. Definition of a High-Confidence Mitochondrial Proteome at Quantitative

Scale. *Cell Rep*. 19:2836–2852. https://doi.org/10.1016/j.celrep.2017.06.014

Narita, M., S. Shimizu, T. Ito, T. Chittenden, R.J. Lutz, H. Matsuda, and Y. Tsujimoto. 1998. Bax interacts with the permeability transition pore to induce permeability transition and cytochrome c release in isolated mitochondria. *Proc. Natl. Acad. Sci. USA*. 95:14681–14686. https://doi.org/10.1073/pnas.95.25.14681

Neginskaya, M.A., J.O. Strubbe, G.F. Amodeo, B.A. West, S. Yakar, J.N. Bazil, and E.V. Pavlov. 2020. The very low number of calcium-induced permeability transition pores in the single mitochondrion. *J. Gen. Physiol*. 152. e202012631. https://doi.org/10.1085/jgp.202012631

Paillard, M., G. Csordás, G. Szanda, T. Golenár, V. Debattisti, A. Bartok, N. Wang, C. Moffat, E.L. Seifert, A. Spät, et al. 2017. Tissue-Specific Mitochondrial Decoding of Cytoplasmic Ca^{2+} Signals Is Controlled by the Stoichiometry of MICU1/2 and MCU. *Cell Rep*. 18:2291–2300. https://doi.org/10.1016/j.celrep.2017.02.032

Paula, S., M. Akeson, and D. Deamer. 1999. Water transport by the bacterial channel alpha-hemolysin. *Biochim. Biophys. Acta*. 1418:117–126. https://doi.org/10.1016/S0005-2736(99)00031-0

Richardson, A.P., and A.P. Halestrap. 2016. Quantification of active mitochondrial permeability transition pores using GNX-4975 inhibitor titrations provides insights into molecular identity. *Biochem. J*. 473:1129–1140. https://doi.org/10.1042/BCJ20160070

Urbani, A., V. Giorgio, A. Carrer, C. Franchin, G. Arrigoni, C. Jiko, K. Abe, S. Maeda, K. Shinzawa-Itoh, J.F.M. Bogers, et al. 2019. Purified F-ATP synthase forms a Ca^{2+}-dependent high-conductance channel matching the mitochondrial permeability transition pore. *Nat. Commun*. 10:4341. https://doi.org/10.1038/s41467-019-12331-1

Wang, Y., N.X. Nguyen, J. She, W. Zeng, Y. Yang, X.C. Bai, and Y. Jiang. 2019. Structural Mechanism of EMRE-Dependent Gating of the Human Mitochondrial Calcium Uniporter. *Cell*. 177:1252–1261.e13. https://doi.org/10.1016/j.cell.2019.03.050

Wolf, D.M., M. Segawa, A.K. Kondadi, R. Anand, S.T. Bailey, A.S. Reichert, A.M. van der Bliek, D.B. Shackelford, M. Liesa, and O.S. Shirihai. 2019. Individual cristae within the same mitochondrion display different membrane potentials and are functionally independent. *EMBO J*. 38. e101056. https://doi.org/10.15252/embj.2018101056